LASER INTERFEROMETER GRAVITATIONAL WAVE OBSERVATORY
-LIGO-
CALIFORNIA INSTITUTE OF TECHNOLOGY
MASSACHUSETTS INSTITUTE OF TECHNOLOGY

Technical Note **LIGO-T000058- 00- R** 5/2/2000

Measurement of Seismic Motion at 40m and transfer function of seismic stacks

D. Ugolini, S. Vass, A. Weinstein

This is an internal working note
of the LIGO Project.

California Institute of Technology
LIGO Project - MS 18-34
Pasadena CA 91125
Phone (626) 395-2129
Fax (626) 304-9834
E-mail: info@ligo.caltech.edu

Massachusetts Institute of Technology
LIGO Project - MS NW17-161
Cambridge, MA 02139
Phone (617) 253-4824
Fax (617) 253-4824
E-mail: info@ligo.mit.edu

WWW: http://www.ligo.caltech.edu/

file /home/ajw/Docs/T000058-00.pdf

Dennis Ugolini
Steve Vass
Alan Weinstein
LIGO Working Document
April 27, 2000
DRAFT 0.93

Measurement of Seismic Motion at 40m and transfer function of seismic stacks

Abstract

In preparation for upgrading the Caltech 40m interferometer for protoyping LIGO II optical configurations, we are measuring the seismic motion of the 40m laboratory and the transfer function of the existing seismic stacks.

1 Introduction

We are attempting to measure the seismic noise and stack transfer functions at the 40m lab. Why?

- Well, just to understand it; learn how to do it, and compare with past measurements [1].
- To evaluate the need for active isolators (STACIS, IDE; we currently think it's a good idea).
- To validate our crude modelling of the stack transfer functions, in order to estimate what they'd be if we replaced the viton with damped metal springs (which we currently think is not advisable).

Guided by the work reported in [2], We will pursue two approaches:

- Use natural ground seismic motion, measure it on the floor and on top of a stack with seismometers, accelerometers, geophones, *etc.*, reading out these instruments with the DAQS system, and analyzing the resulting frames with matlab.
- Use a shaker on the floor or on the stack support bars, and a spectrum analyzer in swept-sine mode to measure the transfer functions.

Currently, we are working on the first approach.

Our equipment:

- We have obtained two 3-axis geophones from MIT. One is typically placed on the floor (in the frames, these signals are called "Floor-X", "Floor-Y", "Floor-Z"), and the other moves around (no matter where it is placed, in the frames, these signals are called "Stack-X", "Stack-Y", "Stack-Z").
- We have a 1-axis seismometer in the lab (in the frames, "IFO-Seis"), which we can orient any way we want.

- We have a small audio microphone (in the frames, "Microphone").

These 8 signals are routed to 8 "spare" fast (16384 Hz) channels in the existing DAQ system, and can be logged to the 40m RAID array when we want to take measurements.

The data are transferred by ftp to a big disk on canopus (a cpu server on the general ligo.caltech.edu sun cluster) and are analyzed with matlab. We know of no way to run matlab on the 40m sun that has the raid array (cdssol9 - albireo) or to mount the raid array on the general ligo.caltech.edu sun cluster.

Calibration: The placard by the seismometer says 340 V/m/s, X20 for the preamplifier gain, for a total of 6800 V/(m/s). The geophone x- and y- coordinates are set to 1000 V/(in/sec) = 39400 V/(m/s). The geophone z-coordinates are set to 100 V/(in/sec) = 3940 V/(m/s). The VME fast ADC (a VMIC3123 16ch, 16-bit, 100kHz S/H ADC running at 16384 Hz) is set to 16384 adc counts / volt. So the final calibration constants are

- IFO-Seis: 1 ADC count = 9.0×10^{-9} m/s
- Geophone x,y: 1 ADC count = 1.6×10^{-9} m/s
- Geophone z: 1 ADC count = 1.6×10^{-8} m/s
- The microphone is in "arbitrary units"...

2 Analysis

- Read in to matlab, 64 seconds of data from all 8 channels, using `frextract`, a matlab function to read frame data (from Benoit Mours' `frame` library, but only in version 3.71, for some reason). We had to modify `frextract` to close the frame file.
- Apply calibration constants to the time series.
- Plot the seismometer time series; look for bumps to see if this is a quiet time.
- Histogram the seismometer time series, and compare with a gaussian with the same mean and σ, to look for non-gaussian seismic noise. Here's an example from the wee hours of the night:

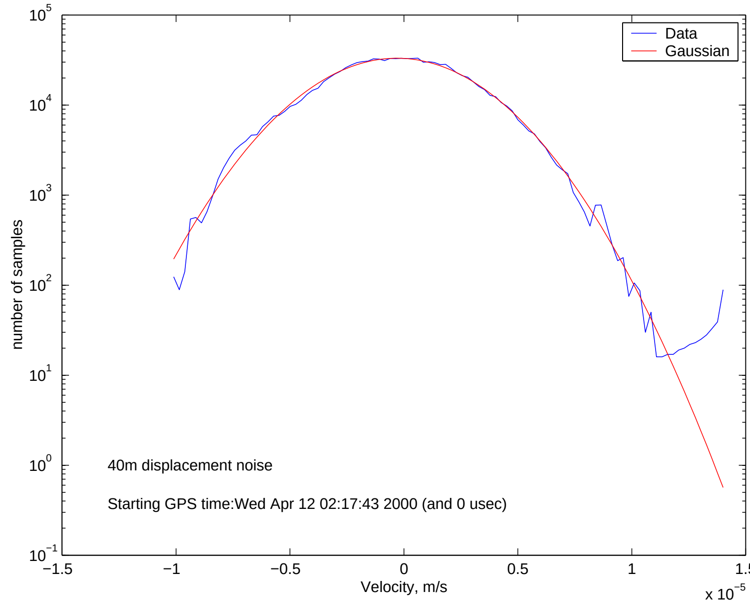

Note that data taken during the day are FAR less gaussian, and have peaks at $\sim 10^{-5}$ m/s. Here are two seismometer time series, one from the day and one at night:

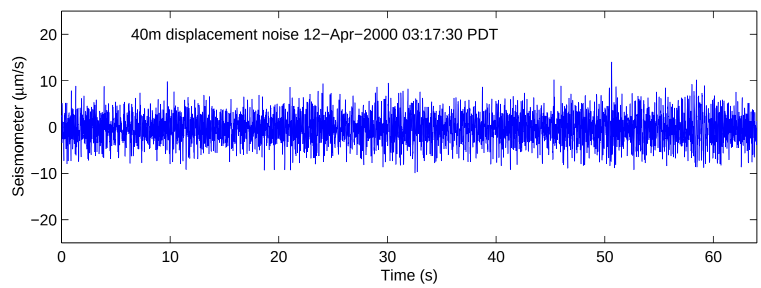

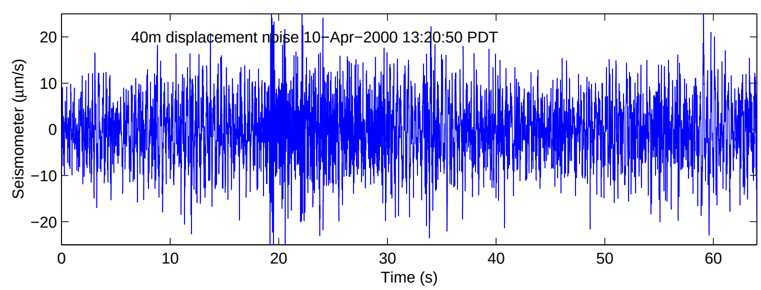

- Take an averaged power spectrum (`pwrsavg` code courtesy of Gabriela): subtract the mean, apply Hanning window, take fft, normalize power spectrum correctly, average 8 sets of 8 consectutive one-second intervals with no overlap.
- Convert from velocity power spectrum to displacement amplitude spectrum, by taking the square root and dividing by $2\pi f$. Here's the result, also from the wee hours, compared with the "noisy Hanford" parameterized spectrum:

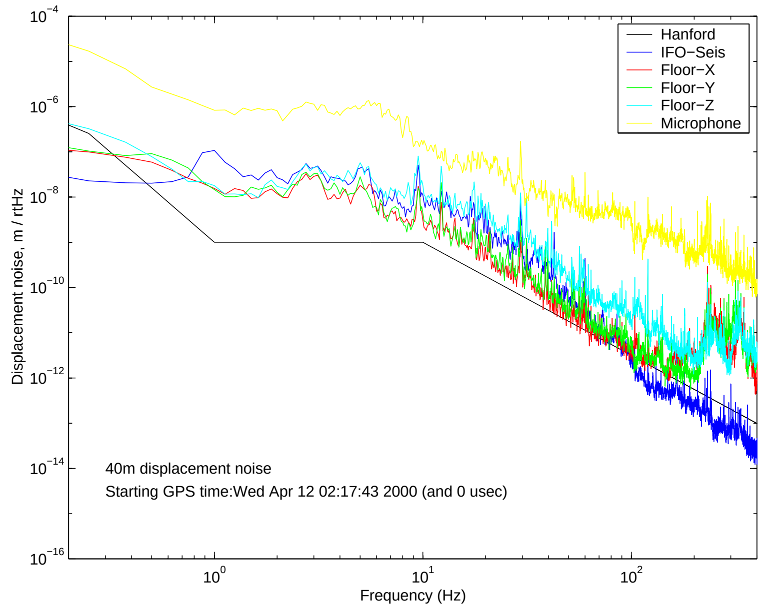

Things to note:

- The seismometer reading compares well with the geophone Z axis.
- The geophone X and Y compare well, and the seismic noise appears to be roughly isotropic.
- The microphone signal has arbitrary units.
- There are spurious resonances in the geophones above 200 Hz, making them useless there.
- The geophones fall off nicely from below 10 Hz to above 100 Hz
- It's not clear why the seismometer reading falls off at 100Hz, since we think the bandpass filter is set to 0.1 – 300 Hz.
- Spectra taken during the day are noisier, but have similar features. Here we compare two spectra taken during the day and at night:

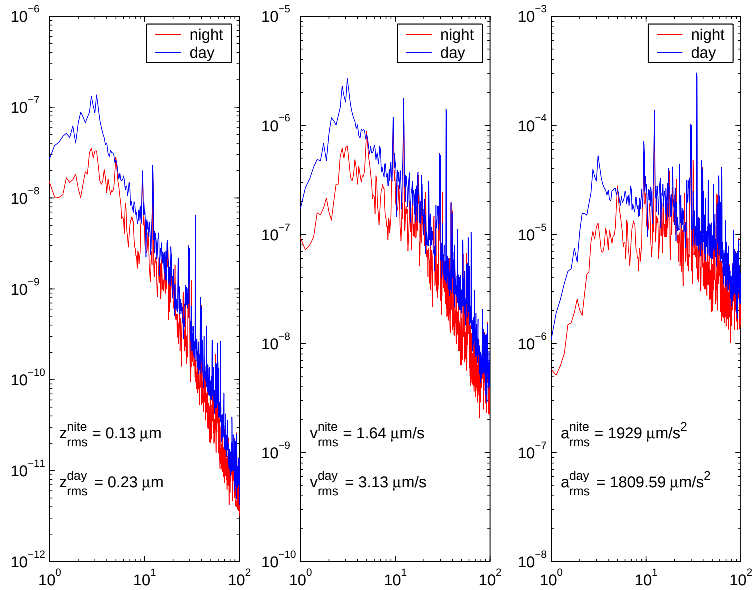

- The spectra are predictably noiser than the "noisy Hanford" parameterized spectrum.
- I have dug up the following plot from the LIGO proposal [1]. Curve B (the 40m lab) compares well with the geophone measurements, including the features at 8 Hz and 22 Hz!

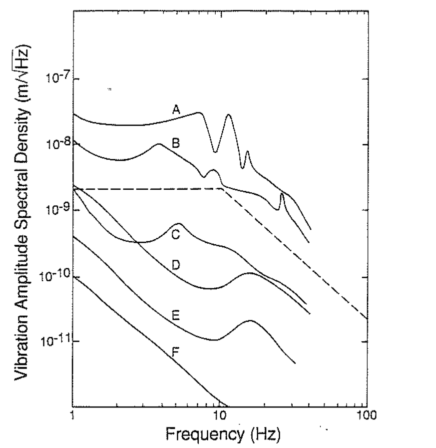

Figure II–3 Vibration amplitude spectral density data for typical motion of the ground at several locations: (A) MIT laboratory; (B) Caltech laboratory; (C and D) potential LIGO sites; (E) Lajitas, Texas (seismically quietest known location in the United States), with 3–10 mph wind conditions; (F) Lajitas, with no wind. The dashed line is the adopted LIGO specification for vibration measured at the instrument mounting structures.

- Calculate the correlation between the different channels (`freqresp` code courtesy of Gabriela): Calculate the average cross spectrum $S_{XY}(f) = \tilde{X}^*(f)\tilde{Y}(f)$ (appropriately normalized); the correlation is $Re(S_{XY})/(|\tilde{X}||\tilde{Y}|)$, and the coherence is $|S_{XY}|^2/(|\tilde{X}|^2|\tilde{Y}|^2)$.

  Here's the result when the geophones are aligned and sitting right next to each other on the floor:

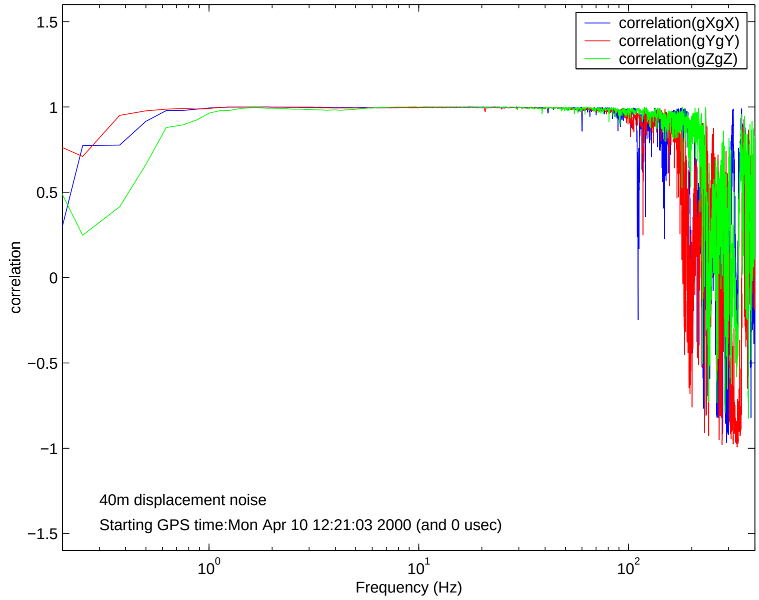

Things to note:

- The fall-off in correlations at ~ 200 Hz, and the (hard to see, but there) anti-correlation at ~ 300 Hz, corresponds to a seismic wavelength of $\lambda_s = v/f = (450 \text{ m/s})/(300 \text{ Hz}) = 1.5$ m or a half-wavelength of 0.75 m, roughly the separation between the geophones.
- There are no evident correlations between other channels, eg, X and Y of the same or different geophones.
- There are weak correlations between the seismometer and the geophone (along the axis which coincides with the seismometer orientation) in the frequency range.

• Divide the displacement power spectrum of the "Stack" geophone by that for the "Floor" geophone, to get the stack transfer function. (Or, take the amplitude of the frequency response of Stack to Floor, $S_{XY}(f)/|\tilde{X}|^2$).

When we do this for the case of both geophones on the floor, the transfer functions are consistent with 1 up to 100 Hz, above which they are dominated by noise.

When we take data with one geophone on top of the EV stack, we get the following plots of the transfer function and the correlations:

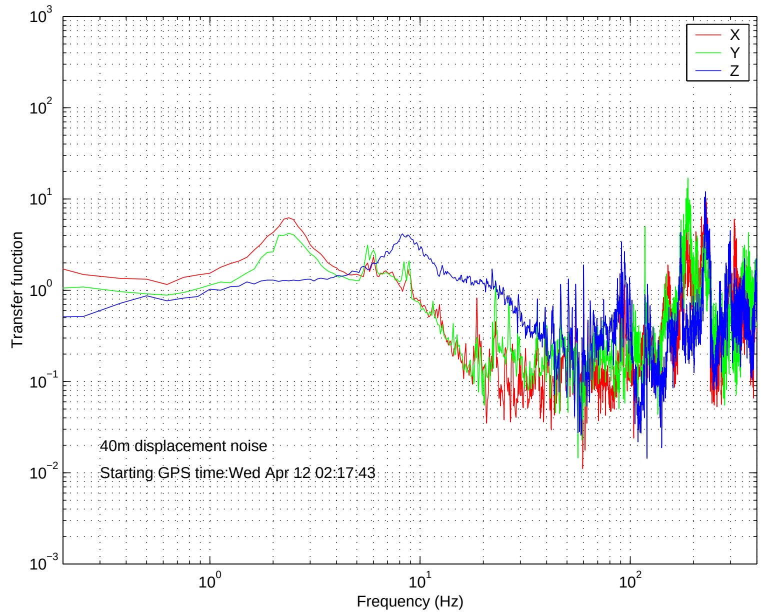

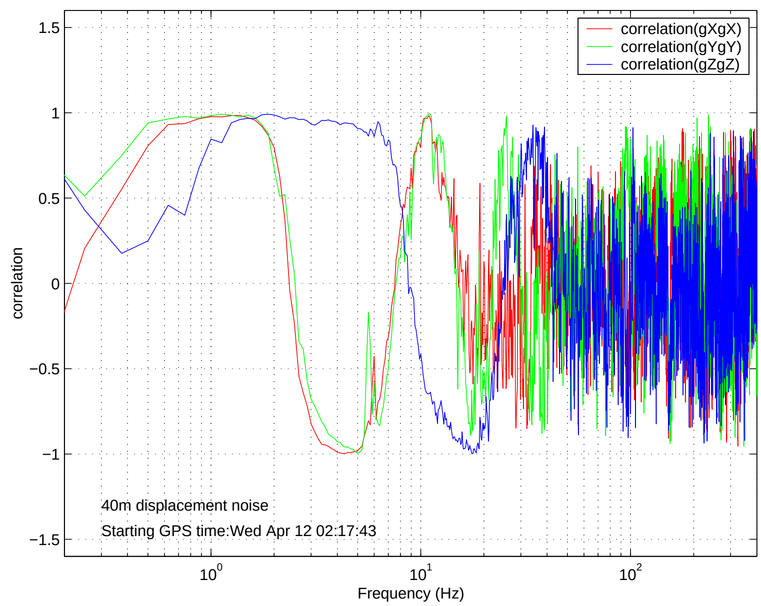

Things to note:

- The resonant peaks are clearly evident. The Z (vertical) peaks at $\sim$ 8.5 Hz, 25 Hz, and 45 Hz are evident as peaks in the transfer function and zero-crossings in the correlation plot. Similarly, for the X and Y resonances at $\sim$ 2.3 Hz, 7.5 Hz, 15 Hz, 22 Hz.
- From Joe Giaime's thesis [7], we know that a 3D FEA model predicts that the horizontal modes have resonant frequencies significantly lower than the vertical ones (see figure below).
- The Z (vertical) peaks are to be compared to my crude model (in which I GUESS at masses and numbers of springs) of 12.0 and 28.9 Hz, 42 Hz, and 61 Hz.
- There appears to be a fall-off from 8 - 12 Hz in the X and Y, but above that, we're not sure what's going on. We're looking to see the sharp $1/f^8$ fall-off between 40-200 Hz.

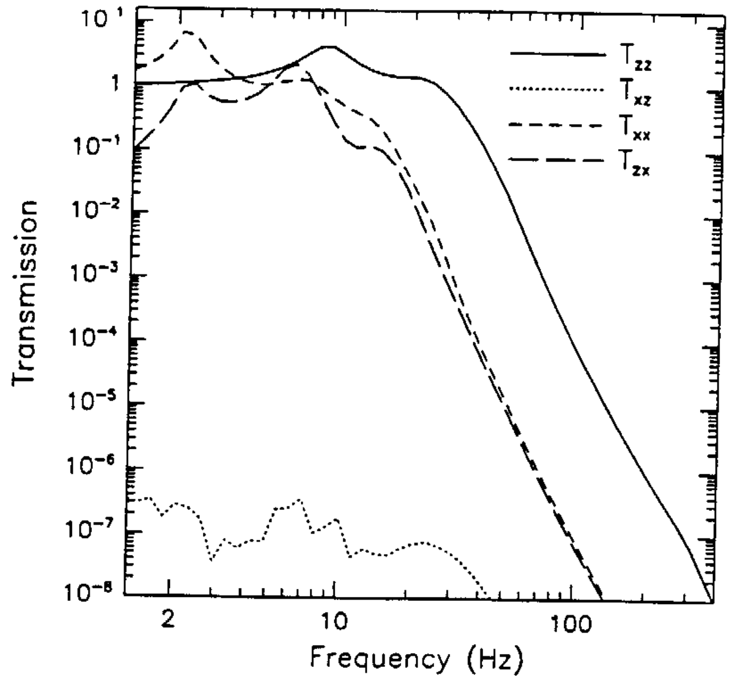

Figure 1: Transfer functions as modelled by symmetric `ABAQUS` model, of a viton stack similar to the 40m. From [7].

3 Transfer functions with the HP spectrum analyzer

We employ the HP 3563A Spectrum Analyzer in swept sine, linear sweep measurement mode. The Source output is fed into the power amplifier of a shaker (ref?), which is tightly clamped to the stack support beam. For measurement of the vertical transfer function, the shaker sits on the floor. For measurement of the horizontal transfer function, the shaker is butted up against a heavy object.

A pair of accelerometers (ref) or geophones is used to measure the transfer function. One rests on the stack support beam, close to the shaker, and the other rests on the top of the seismic stack. The door is closed to minimize air currents, but the system was *not* under vacuum, so acoustic noise is a big problem here.

The Spectrum Analyzer measured the frequency response and coherence, in the range from 10 to 100 Hz, in 800 linear steps, with 4 averages per step. Below 10 Hz, the shaker did not have enough oomph to produce a measurable response on the accelerometer placed next to it; above 100 Hz, there was no coherence in any of the configurations. It took about 5 minutes to complete a measurement.

The results for horizontal and vertical transfer functions, from the accelerometers and geophones, are shown in the following plots.

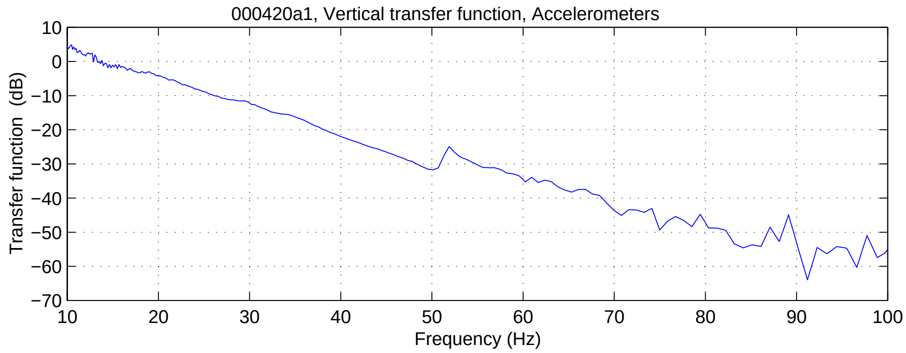
000420a1, Vertical transfer function, Accelerometers
Transfer function (dB)
Frequency (Hz)

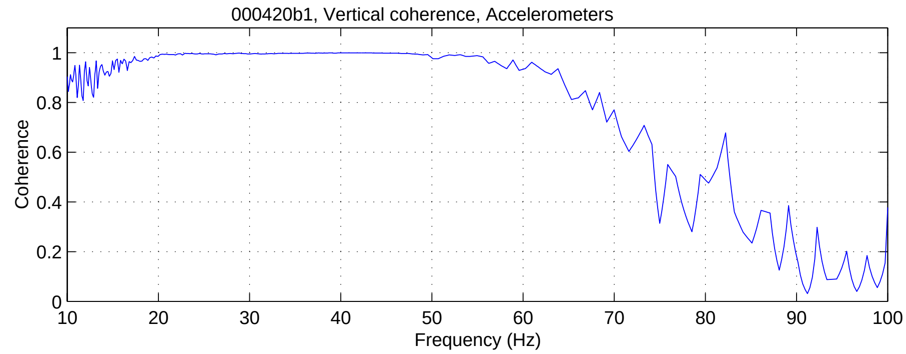
000420b1, Vertical coherence, Accelerometers
Coherence
Frequency (Hz)

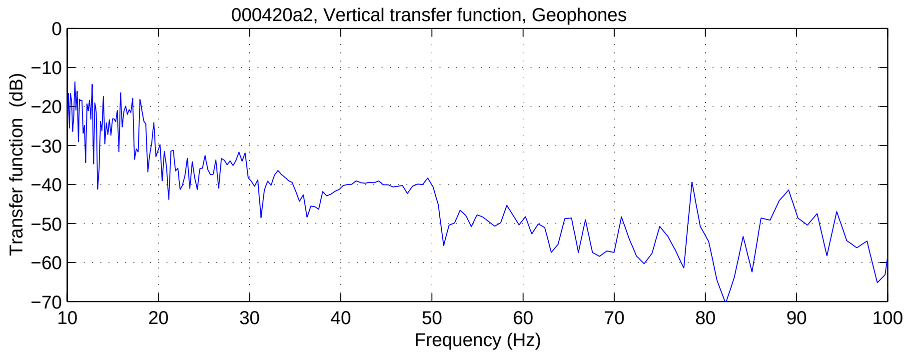
000420a2, Vertical transfer function, Geophones
Transfer function (dB)
Frequency (Hz)

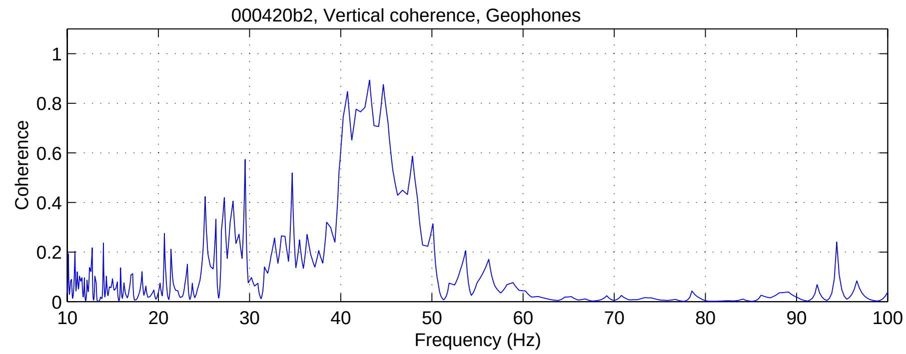
000420b2, Vertical coherence, Geophones
Coherence
Frequency (Hz)

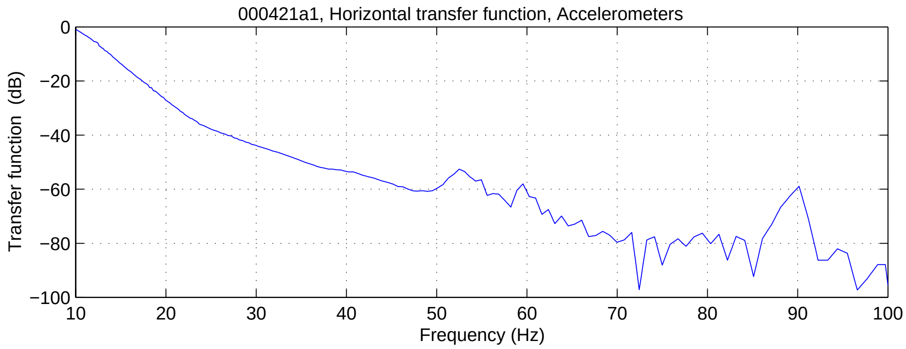
000421a1, Horizontal transfer function, Accelerometers
Transfer function (dB)
0
−20
−40
−60
−80
−100
10 20 30 40 50 60 70 80 90 100
Frequency (Hz)

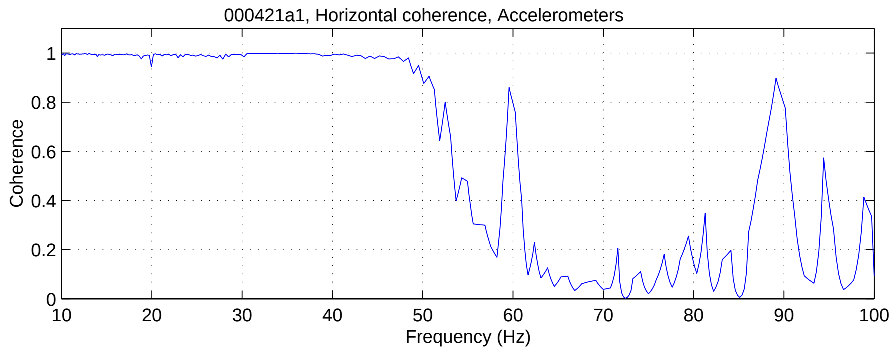
000421a1, Horizontal coherence, Accelerometers
Coherence
1
0.8
0.6
0.4
0.2
0
10 20 30 40 50 60 70 80 90 100
Frequency (Hz)

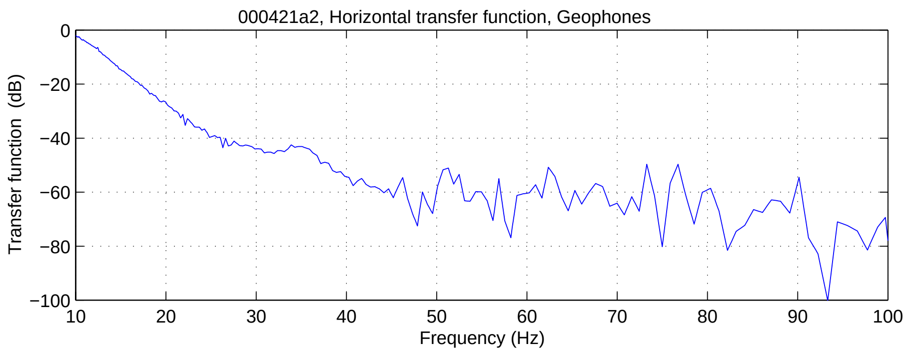
000421a2, Horizontal transfer function, Geophones
Transfer function (dB)
0
−20
−40
−60
−80
−100
10 20 30 40 50 60 70 80 90 100
Frequency (Hz)

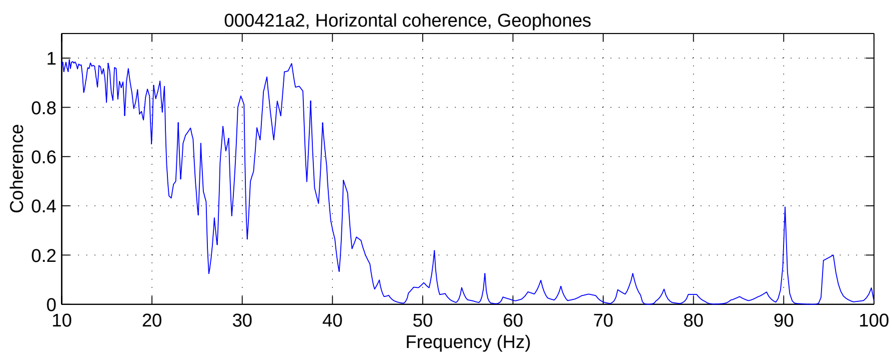
000421a2, Horizontal coherence, Geophones
Coherence
1
0.8
0.6
0.4
0.2
0
10 20 30 40 50 60 70 80 90 100
Frequency (Hz)

We compare the shaker measurements using the accelerometers with the geophone measurements using natural ground motion, and with model calculations incorporating an "eyeball" fit to the observed resonance frequencies, in the following figure:

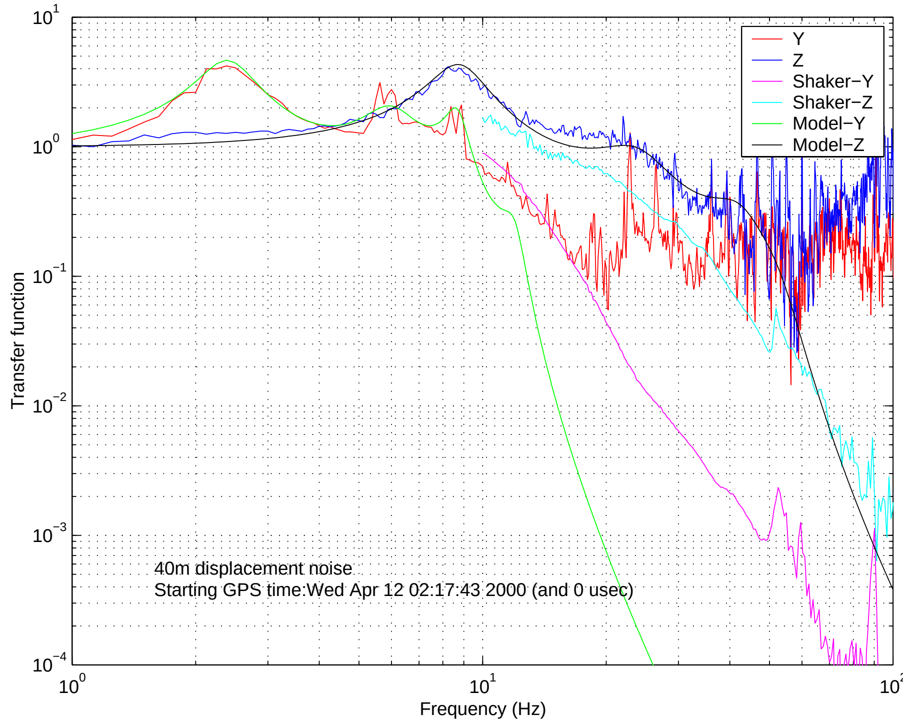

Things to note:

- The geophones are pretty much useless, even in the range (< 40 Hz) where they appear to give reliable data using natural ground motion. (The accelerometers are more-or-less insensitive to natural ground motion). I don't understand this.
- We see that the measured horizontal transfer functions compare well, while the vertical transfer functions are offset. I suspect that the calibration of one of the geophones in the vertical is off; this is under investigation.
- We see that the model of the horizontal transfer function falls far below the measurements, above 10 Hz. This is not understood, but I'm still playing.
- We need to take another transfer function measurement in the vertical, extending down below 8 Hz, despite the weakness of the shaker at such low frequencies.

4 The currently existing stacks

At present, the 40m lab contains five seismic stacks with three legs and four stages, for the chambers housing the beam splitter (BS), south vertex (SV) test mass, south end (SE), east vertex (EV), and east end (EE). There is also an input optics chamber with a square optical table sitting on a one-leg, four stage stack. The layout can be seen in [3].

The three-legged stacks were installed in 4/93. The input optics chamber stack was built in 1996, and installed at the end of that year[4] Engineering drawings for these stacks exist [5].

In each of these stacks, the masses are machined stainless steel, and the springs are viton elastomer.

4.1 The transfer function

To quantify these issues at some level, we have made simple Matlab models of the vertical transfer function

$$T_{zz}(f) = \frac{x_{top}(f)}{x_{floor}(f)}$$

for stacks consisting of all viton springs, all damped metal springs, and mixtures of springs. Foldling these in with the ground motion spectrum $z_{floor}(f)$ allows us to predict the spectrum of motion at the top of the stack, $z_{top}(f)$, and calculate the integrated rms motion x_{rms} and $v_{z,rms}$.

4.2 T_{zz} versus T_{xz} and T_{xx}

For IFO locking and noise performance, the relevant motion is in the direction along the beam (x). However, the stacks are arranged vertically in the local gravitational field, and it is therefore easiest to model the vertical transfer function. The more relevant T_{zx} and T_{xx} transfer functions can only be reliably estimated using 3D finite element analysis tools, which take into account the more complex couplings of z to x, and all the complex properties of all the materials, their shear moduli and geometry, etc.

Fortunately, much work has already been done in this area, by Joe Giaime and others [7]. As summarized in Fig. 1, we see that:

- T_{xz} and T_{xx} have seismic walls at frequencies typically a factor of 2 or more smaller than T_{zz};
- If T_{zz} has a peak at 9 Hz, T_{xz} and T_{xx} peak in the 2 to 3 Hz region, and otherwise lie below T_{zz}.
- These predictions were confirmed (qualitatively) with measurements of a test stack at MIT [7].

This figure can be used to qualitatively extrapolate from a model of T_{zz} to the more relevant T_{xz} and T_{xx}.

4.3 The modelled transfer function

The stacks are designed and modelled as described in the appendix. Here we focus only on the three-legged stacks housing the core optical components; the input and output chamber stacks have similar properties and less critical requirements.

The vertical transfer function T_{zz} is shown in Fig. 2, and the vertical motion at the top of the stack, $z_{top}(f)$, is shown in Fig. 3. In both figures, we show the stacks with all viton springs, all damped metal springs, and a mixture.

The features to note are:

- At high frequencies, all the stack transfer functions have the expected f^{-8} falloff.
- The metal stacks have superior isolation at higher frequencies compared with the viton, with the mixed stacks lying in between. The frequency at which the vertical displacement falls below 1^{-18} m/$\sqrt{\text{Hz}}$ is 39 Hz for metal and 91 Hz for viton.

- The metal stacks have resonant peaks that are less damped and at lower frequencies than the viton stacks, leading to higher peak motion at the resonant frequencies. The viton peaks are all but washed out by the damping.

The numbers used for the springs, all of which probably require confirmation, are summarized in table 1.

The numbers for the stacks are summarized in table 2. Analogous tables for LIGO stacks appear in Ref. [6], and we have checked our calculations against all the numbers in those tables.

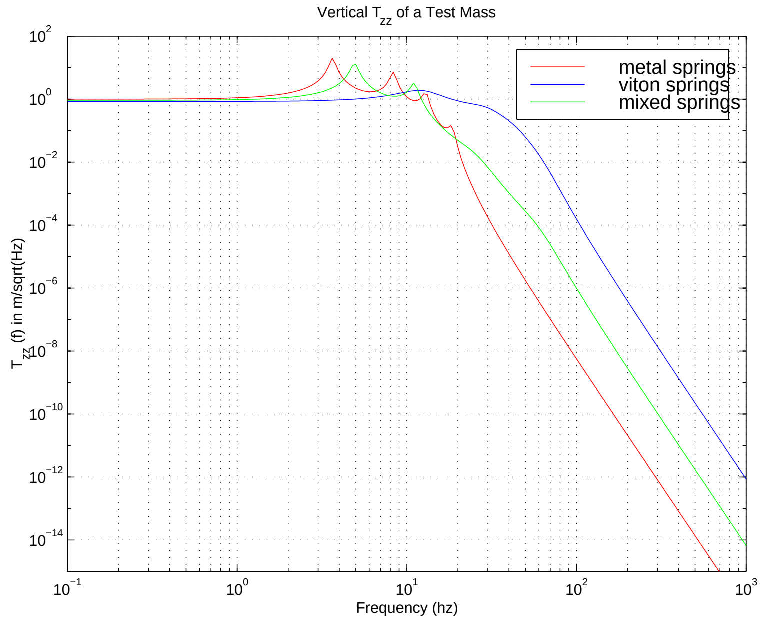

Figure 2: Vertical transfer function T_{zz} (predicted) for 40m seismic stacks built with damped metal springs, viton springs, or a mixture.

Figure 3: Vertical motion $z(f)$ (predicted) for 40m seismic stacks built with damped metal springs, viton springs, or a mixture.

Table 1: Spring parameters.

Spring:	damped metal	viton
k at 100 Hz (Nt/m)	66317	832400
P_{max} (kg)	45	57
η (%)	4	30
Q	25	3.3

Table 2: Stack parameters for 40m three-legged stacks with viton springs, according to these calculations (the reality is to be determined upon disassembly, since we can't find original specifications). The masses and cumulative masses are for the entire stage, summing all three legs. The number of springs $n_{springs}$ is fixed to an integral multiple of 3. The ratio of the actual load to the maximal load borne by the springs is P_{load}/P_{max}. The resonant frequencies of each stage, f_{stage}, is given assuming no couplings between stages, and f_{norm} is from a normal mode analysis of those couplings.

Stage	mass (kg)	cum mass (kg)	$n_{springs}$	P_{load}/P_{max} (%)	f_{stage} (Hz)	f_{norm} (Hz)
Payload	50	50				
4 (top)	173	223	6	66	24.1	12.0
3	275	498	9	98	26.5	28.9
2	275	773	15	91	34.3	42.4
1 (bot)	275	1048	21	88	40.6	60.7
Total springs/stack = 51.						
$\log_{10}(T_{zz})$ at 100 Hz = -3.80.						

5 putting it together

We compare the modelled stack transfer function with the measured one, and with the pendulum transfer function, here:

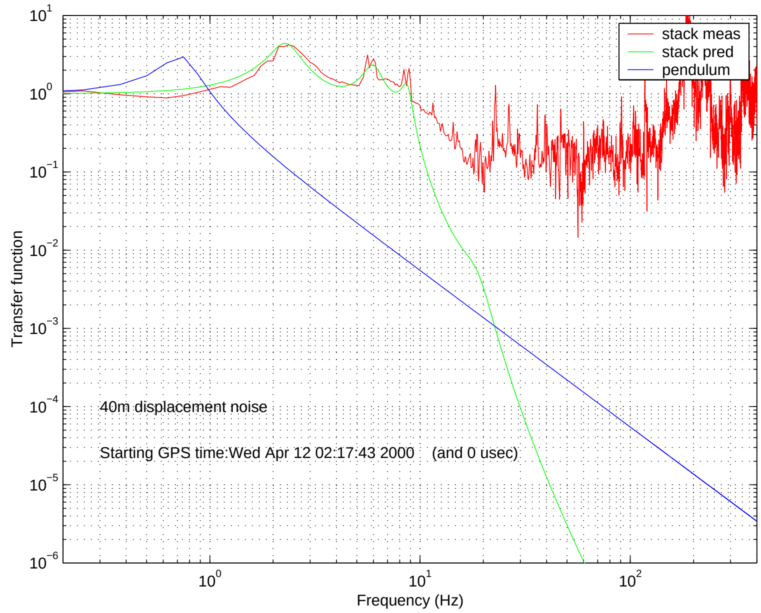

The disagreement above 10 Hz can perhaps be attributed to the inability of the geophones to measure the true motion.

To improve our ability to verify the model at higher frequencies, we will use a shaker to measure the stack transfer function, with a spectrum analyzer in swept-sine mode. This work is in progress.

If we believe the model, from this, we can predict the velocity spectrum at the mirror.

Now we compare the velocity spectrum measured at the floor, with the predicted spectrum at the mirror, using the modelled stack and pendulum transfer functions:

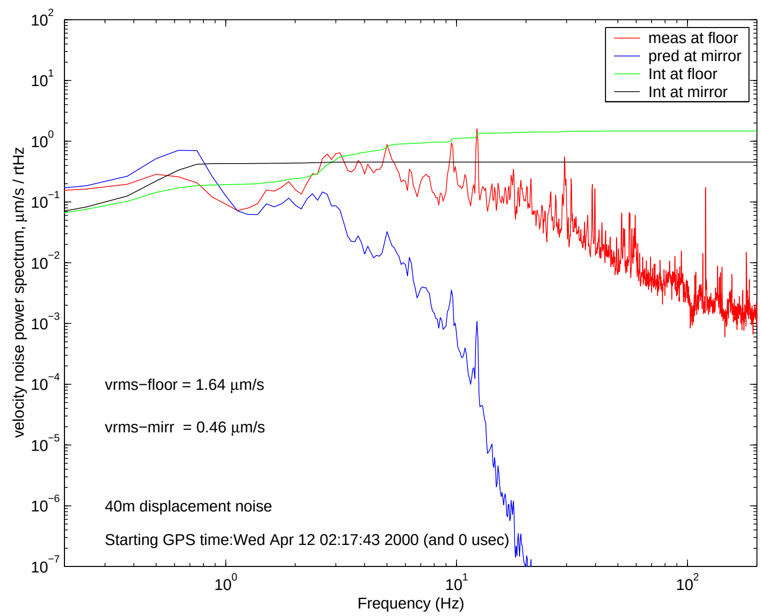

Now we calculate an rms velocity for the two spectra. We verify Parseval's theorem for the velocity spectrum measured at the floor: the standard deviation of the velocity time series is equal to the rms velocity calculated from the power spectrum:

$$v_{rms}^2 = \sum (X(t_i) - \bar{X})^2/N = \sum |\tilde{X}(f_i)|^2 \Delta f$$

OK, the rms velocity on the floor and the mirror are noted in the figure above.

5.1 Mean time to lock

The mean time to lock [8] is given crudely by

$$\tau_{lock} \sim \frac{\lambda/2}{v_{thr} P(v < v_{thr})}$$

where $\lambda = 1.064 \times 10^{-6}$ m, the threshold velocity v_{thr} is the velocity mirror below which the controllers will always acquire lock, and P is the probability, given the mirror velocity distribution, that the velocity is below v_{thr}. The threshold velocity v_{thr} is a complex function of the controller loop gain and bandwidth, but for LIGO it is supposed to be around 1 μm/s or 1 λ/s.

The rms velocity v_{rms} of the mirror as estimated above is on the order of 1 μm/s or 1 λ/s. This compares well with The threshold velocity v_{thr}, so that the mean time to lock is expected to be of order 1s.

To evaluate $P(v < v_{thr})$, we make use of the matlab program `velhist.m`, developed by Gabriela Gonzalez and Brent Ware. We histogram the floor-Y velocity distribution (eventually, we'll fold in the stack and pendulum transfer functions into this calculation),

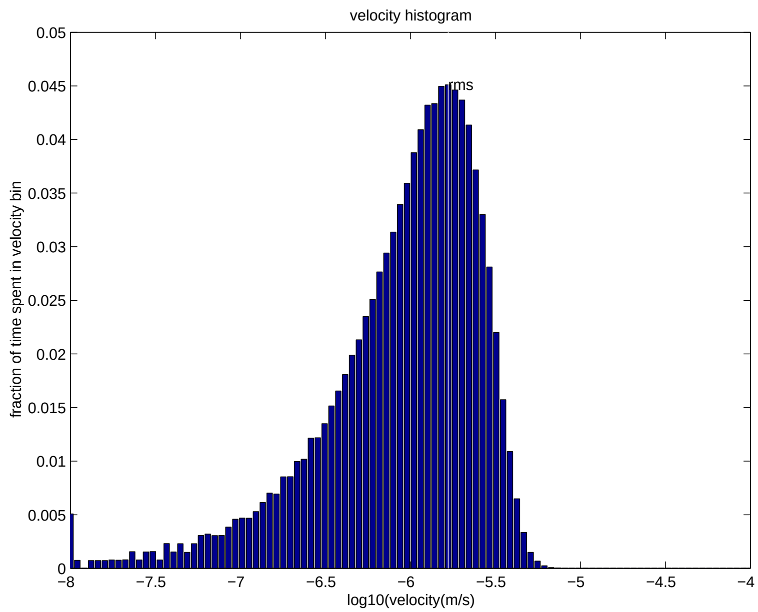

We can compare this distribution (now with a linear x-scale) with idealized curves: The Rayleigh distribution describes the data well.

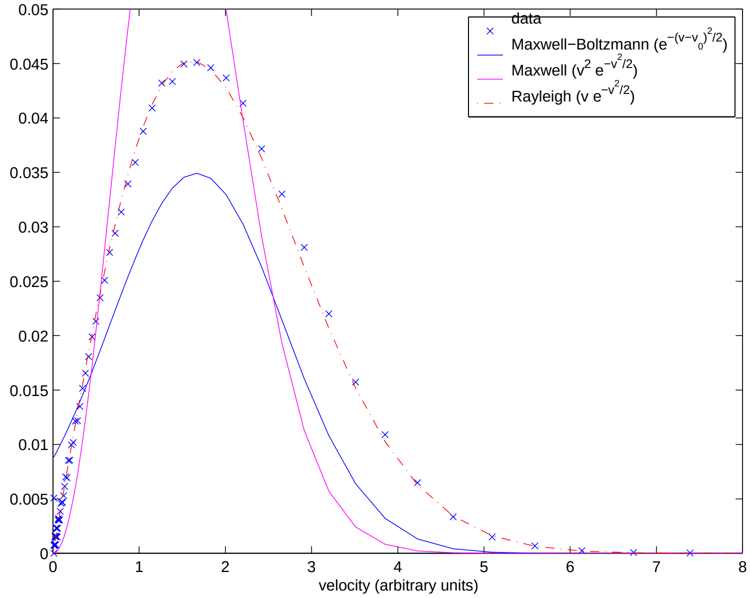

Then we form the cumulative velocity distribution and determine the fraction of time $P(v_{mirr} < v)$ that the mirror velocity falls below v (the x axis).

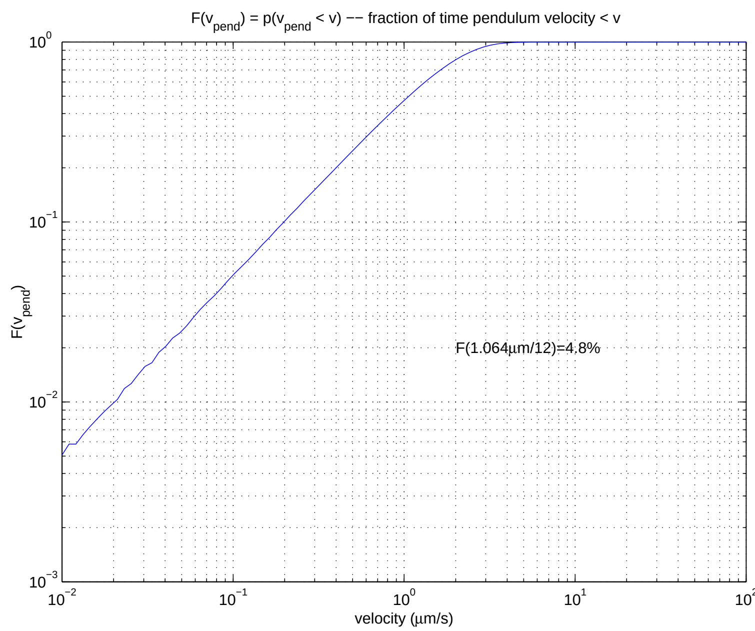

Choosing a threshold velocity of $v_{thr} = 1/12\ \lambda/\mathrm{s}$ (Gaby, why?), we get $P(v_{mirr} < v_{thr}) = 4.8\%$.

6 Summary

Maybe we don't need the active seismic isolator system at all...

However, the ground noise measured during the day can be a factor 10 larger than the quiet spectra in the above figures, as is illustrated above.

7 Acknowledgements

Many thanks to Gabriela Gonzalez, Fred Raab, Joe Giaime, Riccardo DeSalvo and his group, for advice and help.

References

[1] LIGO Proposal to the NSF, LIGO-M890001-00-M.

[2] "Transfer function and drift measurements on the first-article HAM", M. Barton, J. Giaime, G. Gonzalez, W. Johnson, A. Marin. LIGO-T980084-00, 10/98.

[3] LIGO drawing D961304-06: `http://www.ligo.caltech.edu/LIGO_web/dcc/docs/D961304-06.pdf` .

[4] LIGO note M960115-00, `http://www.ligo.caltech.edu/LIGO_web/dcc/docs/M960115-00.pdf` .

[5] LIGO drawings 1205425-1205429, 1205431-1205433, 1205435-1205439, 1205441-1205452, 1202092, 1101012.

[6] E. Ponslet, HYTEC-TN-LIGO-01 (1996); HYTEC-TN-LIGO-02 (1996); HYTEC-TN-LIGO-03 (1996); HYTEC-TN-LIGO-04a (1996); HYTEC-TN-LIGO-07a (1997);

[7] J. Giaime, PhD thesis, MIT (1995); J. Giaime, P. Saha, D. Shoemaker, and L. Sievers, Rev. Sci. Instrum. 67, 208-214 (1996).

[8] "The BIG BOOK of LIGO Lock Acquisition Design", B. Ware, LIGO-T-980666-00-D, 8/98.